

## Measuring membrane protein bond orientations in nanodiscs via residual dipolar couplings

Stefan Bibow,<sup>1</sup> Marta G. Carneiro,<sup>2</sup> T. Michael Sabo,<sup>2</sup> Claudia Schwiegk,<sup>2</sup> Stefan Becker,<sup>2</sup> Roland Riek,<sup>1\*</sup> and Donghan Lee<sup>2\*</sup>

<sup>1</sup>Laboratory for Physical Chemistry, ETH Zürich, CH-8093 Zürich, Switzerland

<sup>2</sup>Department of NMR-Based Structural Biology, Max Planck Institute for Biophysical Chemistry, D-37077 Göttingen, Germany

Received 8 April 2014; Revised 15 April 2014; Accepted 17 April 2014

DOI: 10.1002/pro.2482

Published online 19 April 2014 proteinscience.org

**Abstract:** Membrane proteins are involved in numerous vital biological processes. To understand membrane protein functionality, accurate structural information is required. Usually, structure determination and dynamics of membrane proteins are studied in micelles using either solution state NMR or X-ray crystallography. Even though invaluable information has been obtained by this approach, micelles are known to be far from ideal mimics of biological membranes often causing the loss or decrease of membrane protein activity. Recently, nanodiscs, which are composed of a lipid bilayer surrounded by apolipoproteins, have been introduced as a more physiological alternative than micelles for NMR investigations on membrane proteins. Here, we show that membrane protein bond orientations in nanodiscs can be obtained by measuring residual dipolar couplings (RDCs) with the outer membrane protein OmpX embedded in nanodiscs using Pf1 phage as an alignment medium. The presented collection of membrane protein RDCs in nanodiscs represents an important step toward more comprehensive structural and dynamical NMR-based investigations of membrane proteins in a natural bilayer environment.

**Keywords:** alignment medium; COCAINE; membrane protein; nanodisc; NMR; Pf1 phage; residual dipolar coupling; TROSY

### Introduction

Membrane proteins play key roles in numerous important and complex biological processes. Micelles composed of a variety of detergents have been suc-

cessfully used to study membrane proteins by solution state NMR.<sup>1–4</sup> However, 3D structures determined under these conditions have been challenged since micelles may not mimic a natural membrane environment well often causing a partial loss of their activities.<sup>5</sup> Thus, for NMR structural investigations, other membrane mimetics such as small bicelles composed of a mixture of short-chain and long-chain phospholipids, usually dihexanoyl phosphatidylcholine (DHPC) and dimyristoyl phosphatidylcholine (DMPC) are sometimes used beneficially.<sup>6,7</sup> Another alternative uses phospholipid

Grant sponsor: MPG and an ETH Fellowship (Stefan Bibow).

\*Correspondence to: Roland Riek, Laboratory for Physical Chemistry, ETH Zürich, Wolfgang-Pauli Str. 10, CH-8093 Zürich, Switzerland. E-mail: roland.riek@phys.chem.ethz.ch or Donghan Lee, Department of NMR-Based Structural Biology, Max-Planck Institute for Biophysical Chemistry, Am Fassberg 11, D-37077 Göttingen, Germany. E-mail: dole@nmr.mpiibpc.mpg.de

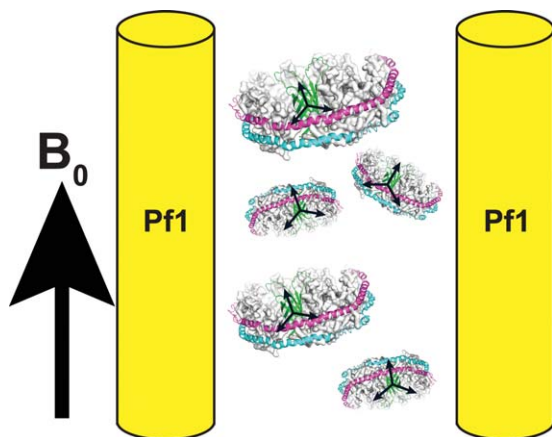


**Figure 1.** Schematic drawing of OmpX-loaded nanodiscs aligned with Pf1 phages. Two Pf1 phages are indicated as yellow cylinders aligned along the labeled static magnetic field of the magnet of the NMR spectrometer. A presumed model of the nanodisc composed of the cyan and pink colored apolipoprotein ApoA-I, the lipid bilayer colored in gray, and OmpX in green are shown. The  $x/y/z$  coordinate system is for each nanodisc indicated highlighting a preferred orientation of the nanodisc and concomitantly the embedded membrane protein OmpX.

nanodiscs (Fig. 1).<sup>8</sup> Nanodiscs are composed of a lipid bilayer surrounded by membrane scaffold proteins (MSPs), for example, apolipoprotein A-I (ApoA-I).<sup>9</sup> Membrane proteins embedded in nanodiscs were successfully studied by various biophysical methods such as force spectroscopy,<sup>10</sup> cryo-EM,<sup>11</sup> fusion assays,<sup>12</sup> and most recently solution state NMR.<sup>13–16</sup> Although nanodiscs mimic physiologic membranes better than micelles, the large overall molecular weight of the systems (150–200 kDa when using native MSPs) hinders their utility for solution NMR studies. Recently, a set of truncated ApoA-I variants were introduced that form smaller nanodiscs, which are suitable for NMR studies of small to medium-sized membrane proteins.<sup>16,17</sup>

Using these smaller nanodiscs an NMR structure of the  $\beta$ -barrel membrane protein OmpX has been determined using secondary chemical shift-based angular restraints,  $\beta$ -sheet hydrogen bonds, and NOEs.<sup>17</sup> Additional structural restraints important for the study of the structure and dynamics of biomolecules can be extracted by residual dipolar couplings (RDCs).<sup>18</sup> The collection of RDCs is in particular essential for the study of membrane proteins due to the scarcity of experimental constraints obtainable for membrane proteins.<sup>18–20</sup> Several alignment media such as neutral<sup>21</sup> and charged gels,<sup>22</sup> DNA nanotubes,<sup>23</sup> lanthanide ions,<sup>24</sup> and bacteriophage fd<sup>25</sup> were successfully used for the studies of membrane proteins in micelles to provide critical structural information. In particular, via the bond orientations obtained from the RDCs through

the alignment, it has been shown that a strong curvature of the HIV-1 Env peptide is induced by micelles.<sup>21</sup> However, till now, there is no reported alignment medium compatible with membrane proteins embedded in nanodiscs. Using the outer membrane protein OmpX from *Escherichia coli* as a model, we show here that membrane protein bond orientations in nanodiscs can be obtained by measuring RDCs using Pf1 phage as an alignment medium.

## Results and Discussions

To establish the measurement of RDCs of a membrane protein localized in nanodiscs, we choose the outer membrane protein OmpX as a model system because <sup>15</sup>N,<sup>13</sup>C,<sup>2</sup>H-labeled OmpX is well studied in various membrane mimics such as micelles,<sup>1</sup> bicelles,<sup>7</sup> and nanodiscs including the small nanodiscs composed of the truncated MSP version MSPΔH5.<sup>17</sup> The alignment medium selected is the bacteriophage Pf1, which was used successfully for the residual alignment of soluble proteins (Fig. 1).<sup>26</sup>

To check the feasibility of the Pf1 phages for the alignment of nanodiscs (Fig. 1), we have added up to 10 mg/mL of Pf1 phages to a solution containing empty nanodiscs composed of the truncated MSP version MSPΔH5<sup>17</sup> and lipids (DMPC and dimyristoylphosphatidylglycine (DMPG)) resulting in a deuterium quadrupolar splitting of D<sub>2</sub>O (5.8 Hz; data not shown). Potential interactions between the empty nanodiscs and the Pf1 phage alignment medium were monitored by chemical shift changes of <sup>15</sup>N-labeled MSP localized in nanodiscs. Although a moderate increase in the line width from <sup>15</sup>N-labeled MSP was apparent for all resonances, no significant chemical shift change in the spectra upon introducing the alignment medium was observed (data not shown), indicating that there is no interaction between the alignment medium and the nanodiscs. Based on the spectral quality of empty nanodiscs, we concluded that, using this approach, the alignment of membrane proteins incorporated into nanodiscs is feasible and may result in high quality spectra.

To show the applicability of this Pf1 phage alignment medium for membrane protein-loaded nanodiscs, the outer membrane protein OmpX was selected. After the reconstitution of OmpX into DHPC micelles, the folding integrity was validated with a [<sup>15</sup>N,<sup>1</sup>H]-TROSY spectrum. Next, the procedure described by Hagn *et al.*<sup>17</sup> was followed for the reconstitution of OmpX into MSPΔH5 nanodiscs composed of lipids (i.e., DMPC and DMPG). The removal of detergents and remaining free lipids is achieved by BioBeads<sup>TM</sup> (BioRad) combined with an extensive dialysis. The latter is useful as DHPC can only be completely removed by dialysis. The overall quality of OmpX reconstituted in nanodiscs assessed

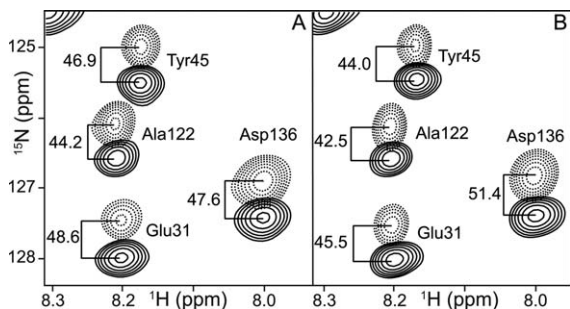


**Figure 2.** RDCs measured in the NMR spectra of deuterated  $^{15}\text{N}$ ,  $^{13}\text{C}$ -labeled OmpX reconstituted in nanodiscs (at a temperature of 318 K in 10 mM Tris-HCl, 100 mM NaCl, 1 mM EDTA, pH 7.4).  $^{15}\text{N}$ ,  $^1\text{H}$ -TROSY (solid lines) and  $^{15}\text{N}$ ,  $^1\text{H}$ -COCAINE (dashed lines) spectra were recorded under (A) isotropic conditions and (B) aligned conditions, which was established by adding 10 mg/mL Pf1 phages into the isotropic sample. In (A)  $0.5 \times {}^1J(\text{HN},\text{N})$  scalar couplings and (B) half of the sum of the scalar coupling and the RDCs of the backbone amide bonds are labeled, respectively. To alleviate severe line broadening due to the size of the system, the experiments were set up in such a manner that the peak position difference between the two spectra give rise to only half of the size of the couplings, that is, scalar and dipolar couplings using  $^{15}\text{N}$ ,  $^1\text{H}$ -COCAINE.

by the  $^{15}\text{N}$ ,  $^1\text{H}$ -TROSY spectrum from our protocol is comparable to that reported by Hagn *et al.*<sup>17</sup> Furthermore,  $^{15}\text{N}$ -resolved  $^1\text{H}$ ,  $^1\text{H}$ -NOESY and TROSY-HNCA spectra were recorded to confirm the published backbone resonance assignment.<sup>17</sup>

For the extraction of RDCs, it is required to record and compare coupling constants both in isotropic (unaligned) and anisotropic (aligned) solution. Although in the isotropic solution only the scalar couplings  ${}^1J(\text{HN},\text{N})$  are present, couplings in the anisotropic solution are a sum of the  ${}^1J(\text{HN},\text{N})$  scalar coupling and the corresponding RDC. Thus, extracting the coupling difference between the two measured spectra provides the desired RDCs. For the scalar couplings of the backbone amide bonds, we first measured  $^{15}\text{N}$ ,  $^1\text{H}$ -HSQC spectra, of which the sensitivity is very poor and which show severe peak overlaps (data not shown) due to the size of the system with an overall tumbling time of 34 ns determined by a TRACT<sup>27</sup> experiment, which is in line with Ref. 17 (data not shown).<sup>17</sup> To alleviate the sensitivity and overlap hindrances, we measured  $^{15}\text{N}$ ,  $^1\text{H}$ -COCAINE<sup>28</sup> spectra that take advantage of the TROSY effect in the  $^1\text{H}$  dimension,<sup>29</sup> whereas the  $^{15}\text{N}$  dimension is recorded in the classical (i.e., non-TROSY) fashion [Fig. 2(A)]. As the  $^{15}\text{N}$ ,  $^1\text{H}$ -COCAINE experiment uses the TROSY effect in the  $^1\text{H}$  dimension, the sensitivity and the spectral crowding could be improved when compared with the corresponding  $^{15}\text{N}$ ,  $^1\text{H}$ -HSQC spectrum (data not shown) and many  ${}^1J(\text{HN},\text{N})$  scalar couplings could be extracted as exemplified for a few residues

in Figure 2(A) (note that the cross peak frequency difference between the  $^{15}\text{N}$ ,  $^1\text{H}$ -TROSY and the  $^{15}\text{N}$ ,  $^1\text{H}$ -COCAINE spectra gives rise to only half of the size of the couplings, i.e., scalar and dipolar couplings).

After obtaining the scalar couplings with the  $^{15}\text{N}$ ,  $^1\text{H}$ -TROSY and the  $^{15}\text{N}$ ,  $^1\text{H}$ -COCAINE spectra, the sample was mixed with 10 mg/mL Pf1 phages to introduce a residual alignment, which was monitored by a deuterium quadrupolar splitting of  $\text{D}_2\text{O}$  (5.8 Hz). The addition of phages showed no significant chemical shift change of the lipid resonances (data not shown). Furthermore, no significant chemical shift change in the  $^{15}\text{N}$ ,  $^1\text{H}$ -TROSY and the  $^{15}\text{N}$ ,  $^1\text{H}$ -COCAINE spectra of OmpX in nanodiscs was observed (exemplified by a comparison of Fig. 2(A) with 2(B)), indicating no significant interaction between the Pf1 phage and the nanodiscs. Also the expected increase of the overall rotational correlation time from the addition of an alignment medium appeared to be not severe: an increase of the rotational correlation time from 34 ns under isotropic conditions to 38 ns in presence of the phage Pf1 was measured by TRACT experiment.<sup>27</sup> Hence, the concomitant proportional increase of the line width of the cross peaks was not too severe either and did not hamper the spectra quality considerably (compare Fig. 2(A) with 2(B)). Therefore, we conclude that Pf1 phages represent a suitable, interaction-free alignment medium for OmpX incorporated in nanodiscs.

Next, following the measurements under isotropic conditions, we collected  $^{15}\text{N}$ ,  $^1\text{H}$ -TROSY and  $^{15}\text{N}$ ,  $^1\text{H}$ -COCAINE spectra of the aligned sample. To obtain RDCs, the extracted couplings between the two spectra detected under anisotropic conditions were subtracted from the corresponding values from the isotropic measurements and then multiplied by 2. Using this protocol, we have obtained 87 backbone  $^1\text{H}$ - $^{15}\text{N}$  bond RDCs ranging from  $-19.8$  to  $23.7$  Hz.

It should be noted that in the case of a significant signal overlap, an alternative route to obtain RDCs for membrane proteins, that is, the TROSY-based 3D-HNCO experiment,<sup>30</sup> can be used.

Figure 3(A) compares these experimentally derived RDCs with the RDCs calculated from the available structure of OmpX reconstituted in nanodiscs, which has been determined without RDCs.<sup>17</sup> Between the observed and the calculated RDCs from the NMR structure, a Pearson's correlation coefficient ( $r$ ) of 0.57 is observed. However, the  $Q$ -value is significantly high ( $Q = 0.81 \pm 0.02$ ), implying that the orientations of N-H bonds are not well defined in the NMR structure.

Finally, we performed a structure calculation of OmpX embedded in nanodiscs using the published experimental restraints derived from NOEs and secondary chemical shifts (Table I) augmented with the

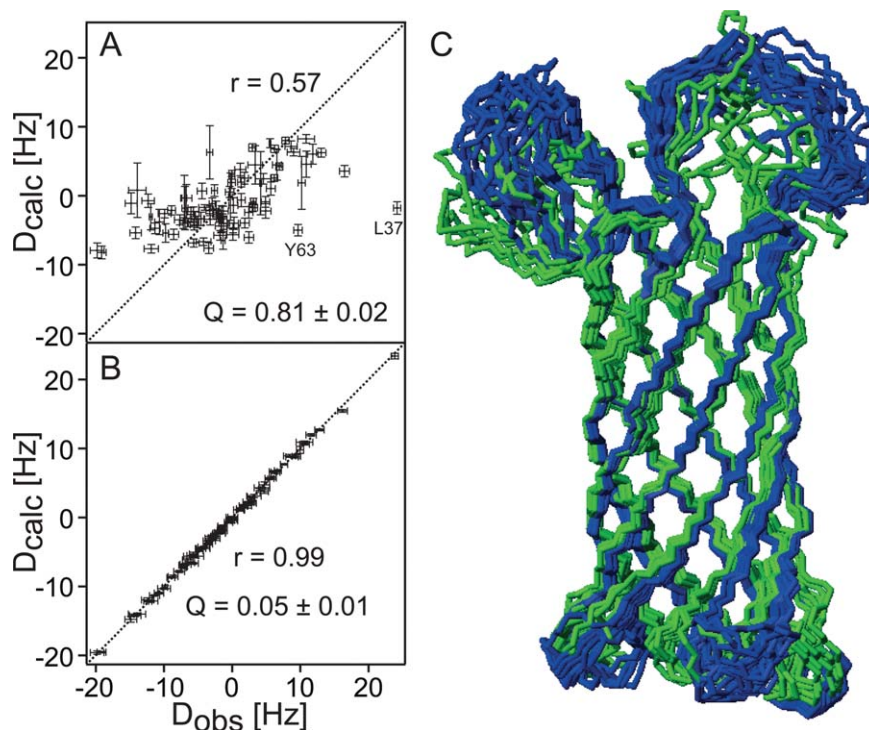


**Figure 3.** Correlation plots between the observed backbone amide bond RDCs and the calculated RDCs from the structures of OmpX determined (A) without (PDB accession code: 2M06) and (B) with RDCs (PDB accession code: 2MNH). (C) Comparison of the 3D structure of OmpX calculated without (blue) and with (green) RDCs. The two structures are represented each by a bundle that fulfills best the experimental input restraints. By introducing the observed backbone amide bond RDCs into the structure determination protocol, the orientations of the backbone amide bonds are significantly improved (compare A with B), as evidenced quantitatively with the Pearson correlation coefficient ( $r$ ) and the quality factor  $Q$  ( $Q = \text{rms}[\text{observed RDC} - \text{calculated RDC}] / \text{rms}[\text{observed RDC}]$ ) listed in A and B.

measured RDCs following established procedures (see Materials and Methods). The calculated 3D structure represented by the 10 conformers that fulfill best the experimental input restraints has a root mean square deviation (r.m.s.d.) of 0.5 Å for the backbone atoms of the secondary structural elements and 1.8 Å for all backbone atoms (Table I, Fig. 3(C)). There are only small residual constraint violations in the final set of the 10 conformers, as well as only small deviations from ideal geometry (Table I). The input data represent therefore a self-consistent set, and the restraints are well satisfied in the calculated conformers. In particular, the RDCs are well satisfied as demonstrated in Figure 3(B) and by the correlation coefficient of 0.99 and the  $Q$ -value ( $0.05 \pm 0.01$ ). Thus, the RDCs have significantly improved the accuracy of the 3D structure including, in particular, much better-defined orientations of the N–H bonds (compare Fig. 3(A) with 3(B)) while the overall structures appear to be similar in terms of RMSD of the secondary structural elements (0.79 Å) (Fig. 3(C)). This finding is expected as using only the backbone amide bond RDCs in the structural determination protocol will not result in dramatic changes in the backbone conformation, but will only provide important orientation information concerning the NH bond within the

peptide plane. Further improvement of the backbone conformation requires the measurement of additional RDCs within the peptide plane such as N–C', N–C $\alpha$ , and C $\alpha$ –C', which are currently being measured by our group.

**Table I.** Experimental NMR Data and Structural Statistics of OmpX Embedded in Nanodiscs

Total number of constraints	424
Total NOE-based distance restraints	58
Total Hydrogen bond constraints	85
Dihedral-angle constraints	194
HN RDC constraints	87
Residual constraint violations	
from all 10 structures	
NOE violation > 0.5 Å	0
Dihedral angle > 5°	0
RDC > 1.5 Hz	1
RMSD Values for	
All backbone atoms	1.8 Å
Secondary structures	0.5 Å
Ramachandran plot for secondary structures <sup>a</sup>	
Most favored regions	98.2%
Additionally allowed regions	1.8%
Generously allowed regions	0.0%
Disallowed regions	0.0%

<sup>a</sup>  $\beta$ -strands residues: 3–14, 20–30, 38–48, 60–71, 78–90, 104–115, 122–132, 135–147.

In summary, we have shown that membrane protein bond orientations in nanodiscs can be obtained by measuring RDCs via Pf1 phages as an alignment medium and using the [<sup>15</sup>N,<sup>1</sup>H]-COCAINE experiment together with the [<sup>15</sup>N,<sup>1</sup>H]-TROSY experiment. As the collection of structural and dynamical restraints is usually limited for membrane proteins, the presented RDC measurements are considered an important additive toward comprehensive structural and dynamical NMR-based investigations of membrane proteins embedded in a lipid bilayer system.

## Materials and Methods

### *OmpX* expression and purification

OmpX was expressed, purified, and refolded in dihexanoyl phosphatidylcholine (DHPC) micelles as described in Lee *et al.*<sup>7</sup> The concentration of OmpX was ~3 mM. The concentration of DHPC (~300 mM) was verified by comparing the 1D <sup>1</sup>H NMR spectrum with the spectrum from a sample containing 100 mM DHPC.

### Expression, purification of MSPΔH5, and reconstitution

Either the plasmid from the Zerbe lab (University of Zurich) originating from and with permission from the Wagner lab (Harvard University) or the synthetically generated plasmid coding MSPΔH5 was used for the expression and purification of MSPΔH5 followed by the procedure described in Hagn *et al.*<sup>17</sup> except the removal of detergents and free lipids, which was done with BioBeads<sup>TM</sup> (Biorad) and simultaneous dialysis (dialysis buffer was 20 mM sodium phosphate, 50 mM NaCl, 5 mM EDTA, pH 6.5). The NMR sample contained 10% D<sub>2</sub>O and 0.01% (w/w) NaN<sub>3</sub>.

### NMR experiments and structure calculation

All NMR spectra were recorded on either a Bruker Avance I or a Bruker Avance III instrument operating at 800 and 900 MHz proton frequency equipped with cryogenic probes at 318 K. TROSY-HNCA and <sup>15</sup>N-resolved [<sup>1</sup>H,<sup>1</sup>H]-NOESY were recorded for controlling the available assignments.<sup>17</sup> For the RDC measurements, [<sup>15</sup>N,<sup>1</sup>H]-TROSY and [<sup>15</sup>N,<sup>1</sup>H]-COCAINE<sup>28</sup> experiments were recorded. All spectra were processed with NMRPipe.<sup>31</sup> Spectral analysis was done with CARA<sup>32</sup> and SPARKY.<sup>33</sup> The program Talos+<sup>34</sup> was used for the prediction of backbone phi and psi angles based on chemical shift data. For the NOESY experiments, a mixing time of 200 ms was used. Structure calculations were done with Xplor-NIH using standard protocols.<sup>35,36</sup> The 10 conformers with the lowest restraint violation energies were used to obtain structural statistics of the ensemble. The constraints used for the structure calculation

and the structures are deposited under RCSB ID code rcsb103826 and PDB ID code 2MNH, respectively. Covalent geometry of the best-energy structure was analyzed with PROCHECK-NMR.<sup>37</sup> The Q-values were calculated using CYANA 3.96<sup>38</sup> and ORIUM.<sup>39</sup>

## Acknowledgments

The authors thank C. Hilty, G. E. Schulz, and K. Wüthrich for providing plasmids used for the production of OmpX. The authors also thank O. Zerbe for the MSPΔH5 plasmid and B. Wicky for initial help with the nanodiscs alignment.

## References

1. Fernandez C, Adeishvili K, Wüthrich K (2001) Transverse relaxation-optimized NMR spectroscopy with the outer membrane protein OmpX in dihexanoyl phosphatidylcholine micelles. *Proc Natl Acad Sci USA* 98:2358–2363.
2. Liang B, Tamm LK (2007) Structure of outer membrane protein G by solution NMR spectroscopy. *Proc Natl Acad Sci USA* 104:16140–16145.
3. Bayrhuber M, Meins T, Habeck M, Becker S, Giller K, Villinger S, Vornrhein C, Griesinger C, Zweckstetter M, Zeth K (2008) Structure of the human voltage-dependent anion channel. *Proc Natl Acad Sci USA* 105:15370–15375.
4. Hiller S, Garces RG, Malia TJ, Orekhov VY, Colombini M, Wagner G (2008) Solution structure of the integral human membrane protein VDAC-1 in detergent micelles. *Science* 321:1206–1210.
5. Sanders CR, Landis GC (1995) Reconstitution of membrane proteins into lipid-rich bilayered mixed micelles for NMR studies. *Biochemistry* 34:4030–4040.
6. Vold RR, Prosser RS, Deese AJ (1997) Isotropic solutions of phospholipid bicelles: a new membrane mimetic for high-resolution NMR studies of polypeptides. *J Biomol NMR* 9:329–335.
7. Lee D, Walter KFA, Bruckner AK, Hilty C, Becker S, Griesinger C (2008) Bilayer in small bicelles revealed by lipid-protein interactions using NMR spectroscopy. *J Am Chem Soc* 130:13822–13823.
8. Bayburt TH, Carlson JW, Sligar SG (1998) Reconstitution and imaging of a membrane protein in a nanometer-size phospholipid bilayer. *J Struct Biol* 123:37–44.
9. Denisov IG, Grinkova YV, Lazarides AA, Sligar SG (2004) Directed self-assembly of monodisperse phospholipid bilayer Nanodiscs with controlled size. *J Am Chem Soc* 126:3477–3487.
10. Zocher M, Roos C, Wegmann S, Bosshart PD, Dotsch V, Bernhard F, Müller DJ (2012) Single-molecule force spectroscopy from nanodiscs: an assay to quantify folding, stability, and interactions of native membrane proteins. *ACS Nano* 6:961–971.
11. Frauenfeld J, Gumbart J, van der Sluis EO, Funes S, Gartmann M, Beatrix B, Mielke T, Berninghausen O, Becker T, Schulten K (2011) Cryo-EM structure of the ribosome–SecYE complex in the membrane environment. *Nat Struct Mol Biol* 18:614–621.
12. Shi L, Howan K, Shen QT, Wang YJ, Rothman JE, Pincet F (2013) Preparation and characterization of SNARE-containing nanodiscs and direct study of cargo release through fusion pores. *Nat Protoc* 8:935–948.

13. Glück JM, Wittlich M, Feuerstein S, Hoffmann S, Willbold D, Koenig BW (2009) Integral membrane proteins in nanodiscs can be studied by solution NMR spectroscopy. *J Am Chem Soc* 131:12060–12061.
14. Raschle T, Hiller S, Yu TY, Rice AJ, Walz T, Wagner G (2009) Structural and functional characterization of the integral membrane protein VDAC-1 in lipid bilayer nanodiscs. *J Am Chem Soc* 131:17777–17779.
15. Tzitzilonis C, Eichmann C, Maslennikov I, Choe S, Riek R (2013) Detergent/nanodisc screening for high-resolution NMR studies of an integral membrane protein containing a cytoplasmic domain. *PLoS One* 8:e54378.
16. Susac L, Horst R, Wüthrich K (2014) Solution-NMR characterization of outer-membrane protein a from *e. coli* in lipid bilayer nanodiscs and detergent micelles. *Chembiochem*. 15:995–1000.
17. Hagn F, Etzkorn M, Raschle T, Wagner G (2013) Optimized phospholipid bilayer nanodiscs facilitate high-resolution structure determination of membrane proteins. *J Am Chem Soc* 135:1919–1925.
18. Bax A (2003) Weak alignment offers new NMR opportunities to study protein structure and dynamics. *Protein Sci* 12:1–16.
19. Tjandra N, Bax A (1997) Direct measurement of distances and angles in biomolecules by NMR in a dilute liquid crystalline medium. *Science* 278:1111–1114.
20. Schwieters CD, Suh JY, Grishaev A, Ghirlando R, Takayama Y, Clore GM (2010) Solution structure of the 128 kDa enzyme I dimer from *Escherichia coli* and its 146 kDa complex with HPr using residual dipolar couplings and small- and wide-angle x-ray scattering. *J Am Chem Soc* 132:13026–13045.
21. Chou JJ, Kaufman JD, Stahl SJ, Wingfield PT, Bax A (2002) Micelle-induced curvature in a water-insoluble HIV-1 Env peptide revealed by NMR dipolar coupling measurement in stretched polyacrylamide gel. *J Am Chem Soc* 124:2450–2451.
22. Cierpicki T, Bushweller JH (2004) Charged gels as orienting media for measurement of residual dipolar couplings in soluble and integral membrane proteins. *J Am Chem Soc* 126:16259–16266.
23. Douglas SM, Chou JJ, Shih WM (2007) DNA-nanotube-induced alignment of membrane proteins for NMR structure determination. *Proc Natl Acad Sci USA* 104:6644–6648.
24. Kamen DE, Cahill SM, Girvin ME (2007) Multiple alignment of membrane proteins for measuring residual dipolar couplings using lanthanide ions bound to a small metal chelator. *J Am Chem Soc* 129:1846–1847.
25. Park SH, Son WS, Mukhopadhyay R, Valafar H, Opella SJ (2009) Phage-induced alignment of membrane proteins enables the measurement and structural analysis of residual dipolar couplings with dipolar waves and lambda-maps. *J Am Chem Soc* 131:14140–14141.
26. Clore GM, Starich MR, Gronenborn AM (1998) Measurement of residual dipolar couplings of macromolecules aligned in the nematic phase of a colloidal suspension of rod-shaped viruses. *J Am Chem Soc* 120:10571–10572.
27. Lee D, Hilty C, Wider G, Wüthrich K (2006) Effective rotational correlation times of proteins from NMR relaxation interference. *J Magn Reson* 178:72–76.
28. Lee D, Vogeli B, Pervushin K (2005) Detection of C' C $\alpha$  correlations in proteins using a new time- and sensitivity-optimal experiment. *J Biomol NMR* 31:273–278.
29. Pervushin K, Riek R, Wider G, Wüthrich K (1997) Attenuated T<sub>2</sub> relaxation by mutual cancellation of dipole-dipole coupling and chemical shift anisotropy indicates an avenue to NMR structures of very large biological macromolecules in solution. *Proc Natl Acad Sci USA* 94:12366–12371.
30. Permi P, Rosevear PR, Annala A (2000) A set of HNCO-based experiments for measurement of residual dipolar couplings in <sup>15</sup>N, <sup>13</sup>C,<sup>2</sup>H-labeled proteins. *J Biomol NMR* 17:43–54.
31. Delaglio F, Grzesiek S, Vuister GW, Zhu G, Pfeifer J, Bax A (1995) NMRpipe—a multidimensional spectral processing system based on unix pipes. *J Biomol NMR* 6:277–293.
32. Keller R (2004) Computer aided resonance assignment. <http://cara.nmr.ch/>.
33. Goddard T, Kneller D (2004) SPARKY 3, University of California, San Francisco.
34. Shen Y, Delaglio F, Cornilescu G, Bax A (2009) TALOS+: a hybrid method for predicting protein backbone torsion angles from NMR chemical shifts. *J Biomol NMR* 44:213–223.
35. Schwieters CD, Kuszewski JJ, Tjandra N, Clore GM (2003) The Xplor-NIH NMR molecular structure determination package. *J Magn Reson* 160:66–74.
36. Schwieters CD, Kuszewski JJ, Clore GM (2006) Using Xplor-NIH for NMR molecular structure determination. *Prog NMR Spectrosc* 48:47–62.
37. Laskowski RA, Rullmann JAC, MacArthur MW, Kaptein R, Thornton JM (1996) AQUA and PROCHECK-NMR: programs for checking the quality of protein structures solved by NMR. *J Biomol NMR* 8:477–486.
38. Güntert P (2004) Automated NMR structure calculation with CYANA. *Methods Mol Biol* 278:353–378.
39. Sabo TM, Smith CA, Ban D, Mazur A, Lee D, Griesinger C (2014) ORIUM: optimized RDC-based iterative and unified model-free analysis. *J Biomol NMR* 58:287–301.